Dynamic Two-Center Interference in High-Order Harmonic Generation from Molecules with Attosecond Nuclear Motion

S. Baker,[1] J. S. Robinson,[1] M. Lein,[2] C. C. Chirilă,[2] R. Torres,[1] H. C. Bandulet,[3] D. Comtois,[3] J. C. Kieffer,[3] D. M. Villeneuve,[4] J. W. G. Tisch,[1] and J. P. Marangos[1]

[1]*Department of Physics, Imperial College London, London, SW7 2AZ, United Kingdom*
[2]*Institute of Physics, University of Kassel, Heinrich-Plett-Strasse 40, 34132 Kassel, Germany*
[3]*INRS-Centre Énergie, Matériaux et Télécommunications, 1650 Lionel-Boulet, Varennes, Québec, J3X 1S2, Canada*
[4]*National Research Council of Canada, 100 Sussex Drive, Ottawa, Ontario, K1A 0R6, Canada*

(Received 24 September 2007; revised manuscript received 22 November 2007; published 30 July 2008)

We report a new dynamic two-center interference effect in high-harmonic generation from H_2, in which the attosecond nuclear motion of H_2^+ initiated at ionization causes interference to be observed at lower harmonic orders than would be the case for static nuclei. To enable this measurement we utilize a recently developed technique for probing the attosecond nuclear dynamics of small molecules. The experimental results are reproduced by a theoretical analysis based upon the strong-field approximation which incorporates the temporally dependent two-center interference term.

DOI: 10.1103/PhysRevLett.101.053901 PACS numbers: 42.65.Ky, 33.15.Dj, 42.65.Sf

High-harmonic generation (HHG) has proven to be a rich area of study over the last decade, finding application in areas such as coherent x-ray production [1,2], attosecond pulse generation [3–5], and time resolved probing of nuclear dynamics [6,7]. HHG has also led to important advances towards the structural imaging of small molecules [8–15], the harmonic emission depending on the nature of the molecular orbital involved. This is seen most clearly within the strong-field approximation (SFA), in which the amplitude for HHG is determined by the Fourier transform of the bound state wave function.

The wave functions relevant to HHG are those describing the propagated continuum electron (ψ_c), and the bound electronic state from which the electron was ionized (ψ_g). Interference between ψ_c and ψ_g on recollision of the electron wave packet with its parent ion results in an oscillating dipole ($\langle\psi_c|r|\psi_g\rangle$) being induced on the molecule as the probability distribution of the electron density around the nuclei ($|\psi_c + \psi_g|^2$) varies during the recollision. It is the acceleration of this dipole which is responsible for harmonic emission. Within this picture, suppression of harmonic emission occurs if the shape, size, and symmetry of ψ_c and ψ_g are such that only a weak net oscillating dipole is induced on the molecule. For example, for a diatomic molecule with a symmetric ψ_g, the dipole induced at each molecular center oscillates precisely out of phase if $2R\cos(\theta) = \lambda$ [8], where R is the molecular internuclear separation, θ is the angle between the molecular axis and the electric field of the driving laser, and λ is the de Broglie wavelength of the returning electron. Destructive interference is thus a result of a resonance in the electronic dipole term, being first predicted in H_2 and H_2^+ molecules in 2002 [9]. To date this effect has been observed experimentally in CO_2 [13,14], but not in H_2.

Here we report the observation of a new kind of two-center interference, in which the nuclear dynamics launched at ionization play a critical role. In previous studies, the molecular nuclei have been considered static, and the chirp of the returning electron wave packet largely ignored. We now show that in a system with fast moving nuclei (H_2), the interference occurs in a transient fashion involving a dynamic matching of the molecular internuclear separation and the recolliding electron wavelength.

To enable this measurement, we have used a recently developed technique termed PACER (probing attosecond dynamics by chirp encoded recollision) which allows the nuclear dynamics following ionization to be probed with a temporal resolution of roughly 100 as [6]. The essence of PACER is the sensitivity of the harmonic signal to changes in the nuclear part of the wave function $\chi(R, t)$ during the excursion time of the electron τ, through the nuclear autocorrelation function $c(\tau) = \int \chi(R, 0)\chi(R, \tau)dR$. $c(\tau)$ (and thus the harmonic signal) decreases the more the nuclei move in the small time interval τ [6,16]. In addition, since different harmonic orders correspond to different values of τ [17], a single recollision probes the nuclear wave packet at a range of times. Each harmonic spectrum therefore has within it details of the nuclear motion, which can be revealed on comparison of harmonic signals in different isotopes of a molecular species: it has been shown that the ratio of harmonic emission in D_2 and H_2 increases with harmonic order (or τ) [6], since at longer times the *difference* in the internuclear separation of H_2 and D_2 increases.

PACER offers the attosecond resolution necessary to observe *dynamic* two-center interference. However, in previous measurements the harmonic signal was predominantly sensitive to the nuclear part of the wave function, through $c(\tau)$ [6]. The electronic contribution was largely insignificant [18] because the measurement was made in a

randomly aligned sample. To allow the observation of dynamic interference, we enhance the sensitivity to the electronic part of the wave function by employing longer and more intense driving pulses, to produce a significant degree of alignment by the driving pulse itself.

This work was conducted at the Advanced Laser Light Source (ALLS) in Quebec, Canada. The 800 nm, 30.0 ± 0.5 fs pulse was diagnosed using a Thales 6800913A autocorrelator at a position equivalent to the interaction region. Previous measurements showed the pulse contrast to be 10^3 within 200 fs of the pulse, and $>10^6$ over 10 ps. The beam was focused by an $f = 400$ mm lens beneath a pulsed gas jet, the repetition rate of which was limited to 4 Hz by the pressure in the detection chamber. The gas jet had previously been characterized so as to deliver H_2 and D_2 to the interaction region at a constant density ($\pm 14\%$). The confocal parameter of the focused beam was measured as 5.5 mm; the path through the jet is estimated to be 0.5 mm. The focus was positioned 4 mm before the jet to ensure that short electron trajectories dominated the harmonic signal [19] (achieving a unique time to frequency mapping). The rms variation in pulse energy ($\sim 2\%$) was monitored during each data run. The generated signal was resolved by a spectrometer, and measured by an imaging MCP, phosphor screen, and CCD camera.

Single-shot spectra were observed for a range of driving field intensities. The on-target intensity was determined from the position of the harmonic cutoff (corresponding to $3.17U_p + I_p$), ensuring that the value stated is that of the part of the beam dominating the emission of the harmonics detected. The error in intensity was found by considering the increase needed to generate one more order than was observed. Intensity values determined in this way are within 30% of those determined from energy and spot size readings. Preliminary measurements were made to ensure that harmonic emission was not saturated.

Figure 1 shows the measured ratio of harmonic signals in D_2 and H_2 at two driving field intensities: $(3.0 \pm 0.1) \times 10^{14}$ W cm^{-2} and $(2.2 \pm 0.2) \times 10^{14}$ W cm^{-2}, plotted against the calculated electron travel time τ corresponding to each harmonic order [16]. The average signal ratio was computed over 500 single-shot spectra in each gas, with error bars representing the standard error. We have confirmed that comparison of the signal in two experimental runs in the same gas yields a harmonic ratio that is constant with τ. However, for $\tau > \sim 1.5$ fs there are large errors, and the ratio of signals in, e.g., $H_2 : H_2$ begins to deviate strongly from a constant value. This is because large τ are associated with very weak emission in the harmonic cutoff, where the signal to noise ratio is poor, and the ratio is extremely sensitive to the background level used (a 0.2% change in the background level is found to shift the two data points at highest τ by $\sim 10\%$ and 30%, respectively, while leaving other data points unaffected).

Over the range of τ for which the experimental data is reliable a clear trend is seen: the harmonic ratio increases

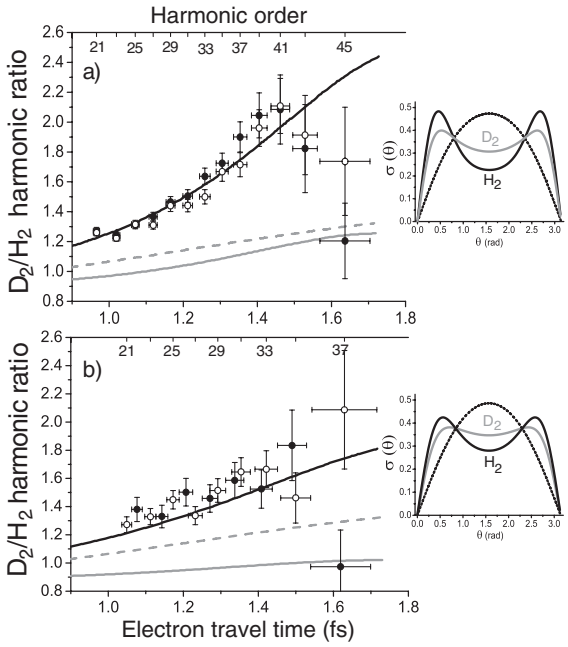

FIG. 1. (a) Measured ratio of harmonic signals in D_2 and H_2 at driving field intensity $(3.0 \pm 0.1) \times 10^{14}$ W cm^{-2}. Two independent data sets are shown. Black line shows prediction from SFA calculation [Eq. (2)]. Gray line shows SFA calculation in which the nuclear motion has been neglected. Dotted line shows SFA calculation in which two-center interference is neglected. Inset shows calculated alignment distribution $\sigma(\theta)$ [20] at the pulse peak in H_2 and D_2 at this intensity. For comparison the dotted curve shows $\sigma(\theta)$ for the 8 fs case investigated in Ref. [6]. (b) Same as (a), but for driving field intensity $(2.2 \pm 0.2) \times 10^{14}$ W cm^{-2}.

with τ for both driving field intensities, but this increase is more significant at the higher driving field intensity, the difference between the data at the two intensities becoming more pronounced for longer τ.

The driving field intensity affects HHG through both the momentum evolution of the returning electron wave packet and the alignment distribution of the sample at the peak of the driving pulse. Both of these factors affect the conditions for two-center interference, and thus we investigate if this is responsible for the faster growth in harmonic ratio with τ observed for the higher driving field intensity case. However, in this system we must consider the interference as a *dynamic* process, occurring when the internuclear separation of the expanding nuclear wave packet passes through a value that matches the returning electron wavelength *at that time*. We therefore define a simple condition for destructive interference in this dynamic system as $2R(t)\cos(\theta_m) = \lambda(t)$, where θ_m is the modal value of the alignment distribution $\sigma(\theta)$ at the peak of the pulse, calculated by the method detailed in [20]. Here sech^2 pulses of FWHM 30 fs and peak intensities 3.0×10^{14} W cm^{-2} and 2.2×10^{14} W cm^{-2} are used to calculate the evolution of $\sigma(\theta)$ under the pulse envelope. The alignment distribution at the moment of HHG is assumed to be that at the peak of

the pulse (Fig. 1 insets). This calculation has been shown to yield accurate results when compared to measured alignment distributions at similar intensities [21]. We find that the experimental error in intensity leads to an error of only $\sim 1\%$ in the value of $\cos^2(\theta)$.

We then plot in Fig. 2 $2R(t)\cos(\theta_m)$ for H_2^+ (solid line, where $R(t)$ is the average value of the expanding nuclear wave function, calculated as in [16]) and the returning electron wavelength λ as a function of τ (data points) for the appropriate experimental conditions, using the relationship $\lambda = h(2m_e n\hbar\omega)^{-0.5}$ [13], where m_e is the electron mass, ω is the driving laser frequency, and n is the harmonic order. A point of intersection of these two curves thus represents suppression of H_2 harmonic emission at the harmonic order corresponding to the instantaneous electron wavelength at the time of intersection. In Fig. 2 we also plot $2R_{eq}\cos(\theta_m)$, where R_{eq} is the equilibrium separation of the H_2 molecule (1.4 a.u).

Figure 2 shows that the two driving field intensities employed are indeed in different two-center interference regimes: for the high driving field intensity this simple model predicts that destructive interference may occur in H_2 around the 39th harmonic order emitted 1.4 fs after ionization, whereas for the low intensity case, destructive interference is not predicted to occur. Further, for an intensity of $(3.0 \pm 0.1) \times 10^{14}$ W cm^{-2}, destructive interference is not expected to occur if one neglects the nuclear dynamics (dotted line), which are a necessary condition for suppression of H_2 harmonics to occur. A new *dynamic* two-center interference effect is therefore introduced, as represented schematically in Fig. 3. If this simple analysis is repeated for D_2, one finds that the condition for destructive interference is not satisfied for our experimental conditions. The signature of the dynamic interference in this system will thus be the observation of higher values for the ratio of harmonic signals in D_2 and H_2, as emission is suppressed in H_2 only. Our measurements (Fig. 1) are thus in qualitative agreement with such an effect, since we detect elevated signal ratios for the high intensity case as compared to the lower intensity case.

We note that destructive two-center interference normally gives a dip in the harmonic spectrum [13] centered around the order corresponding to the wave packet component which best satisfies $2R\cos(\theta) = \lambda$. For our experimental conditions this is the 39th harmonic order (see Fig. 2). Since this is very high in the cut-off region of the spectrum, we do not generate enough harmonic orders to clearly observe the dip, and the interference is manifested in our experimental data only as an increase in the ratio of the harmonic signals (D_2/H_2) for higher orders.

To test further whether a dynamic two-center interference effect could play a significant role, we perform calculations of HHG in a simplified strong-field approximation, including the known internuclear dynamics of H_2^+ and D_2^+, and the effect of two-center interference. If ψ_c is described as a superposition of plane waves of amplitudes $a(k)$, [$\psi_c = \int a(k)e^{ikx}dk$], the harmonic signal at frequency ω is proportional to $\omega^2|a(k)v(k)|^2$ [11], where the recombination amplitude $v(k)$ in the case of a molecule can be formulated as [22]

$$v(k) = \int \chi_0(R)\langle\Psi_0(R)|k|e^{ikx}\Psi_0^+(R)\rangle\chi(R, \tau(k))dR, \quad (1)$$

$\Psi_0(R)$ and $\Psi_0^+(R)$ being the electronic ground states of the neutral molecule and ion, respectively, and $\chi_0(R)$ and $\chi(R, \tau)$ the initial and propagated nuclear wave packets

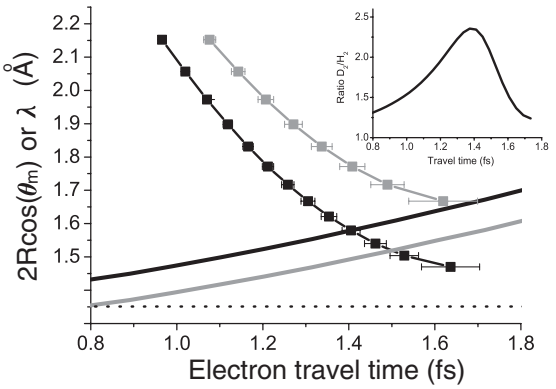

FIG. 2. Data points show electron wavelength corresponding to the harmonic orders observed at driving field intensities of $(3.0 \pm 0.1) \times 10^{14}$ W cm^{-2} (black) and $(2.2 \pm 0.2) \times 10^{14}$ W cm^{-2} (gray), plotted against electron travel time. Solid lines show $2R(t)\cos(\theta_m)$ for H_2^+ at the high (black) and low (gray) intensities. Dotted line shows $2R_{eq}\cos(\theta_m)$ for H_2 at an intensity $(3.0 \pm 0.1) \times 10^{14}$ W cm^{-2}. Inset shows SFA calculation of signal ratio at 3.0×10^{14} W cm^{-2} assuming a single alignment angle θ_m.

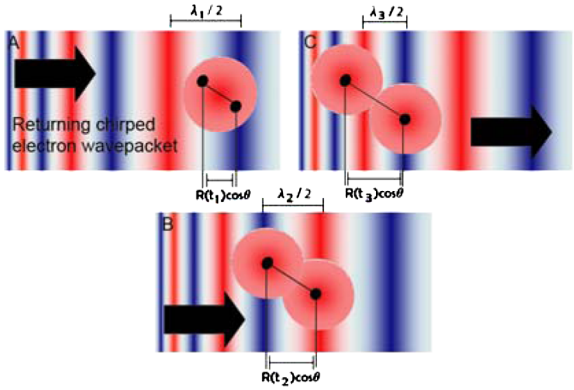

FIG. 3 (color online). *Dynamic* two-center interference in HHG, considering a chirped returning electron wave packet ($\lambda_1 > \lambda_2 > \lambda_3$) and an evolving nuclear wave function. Red and blue represent opposite signs of the wave functions. At early times (A) and late times (C), the condition for two-center interference is not satisfied [$2R(t_1)\cos\theta \ll \lambda_1$, $2R(t_3)\cos\theta \gg \lambda_3$]. The corresponding low and high-order harmonics are therefore emitted without significant interference. At intermediate times (B), $2R(t_2)\cos\theta \approx \lambda_2$, and thus the emission of harmonics of photon energy $h/2m\lambda_2^2$ is suppressed.

in the molecular ion. R-independent factors $r(k)$ can be removed as prefactors to this integral to yield $v(k) = r(k)c_\theta(k)$ with [22]

$$c_\theta(k) = \int \chi_0(R)\chi[R, \tau(k)]\cos[kR\cos(\theta)/2]dR, \quad (2)$$

which is then averaged over the relevant distribution of alignment angles (calculated as described earlier in text). Assuming isotopic invariance of $a(k)$, the ratio of harmonic signals in an isotope pair thus reduces to the modulus squared of the ratio of $c_\theta(k)$ in each isotope. Since the tunneling ionization rates of H_2 and D_2 (proportional to $\exp[-2(2I_p)^{3/2}/3E]$ [23]) differ by $<3\%$ for these conditions, and the shape of $a(k)$ in atoms has been shown to be insensitive to large changes in I_p [24], isotopic invariance of $a(k)$ is a reasonable assumption. The ratio of harmonic signals calculated by this method is shown in Fig. 1. We also show calculations in which two-center interference is neglected by dropping the cosine term, and in which the nuclei are considered fixed [$\chi(R, \tau) = \chi_0(R)$]. To allow for the experimental error in gas density, all calculations shown in Fig. 1 have been scaled by a small factor (0.85). In separate calculations we have investigated the effect of the coupling between the laser field and the molecular ion, and found that this has only a small effect on the predicted ratios. Therefore we neglect this effect in the calculations presented in Fig. 1.

It can be seen from Fig. 1 that the SFA calculation predicts that higher ratios are obtained for the high intensity as compared to the low intensity case, and that this effect is more pronounced as τ increases. The SFA calculation is therefore in qualitative agreement with the simple model presented in Fig. 2. There is also excellent quantitative agreement between the experimental data and the SFA calculation for both intensity regimes. In addition, it can be seen from Fig. 1 that if either the nuclear motion or the effect of two-center interference are neglected from the calculation, the agreement with the experimental data is lost. This confirms that what we observe is a *dynamic* two-center interference effect in HHG in H_2, in which the nuclear motion is crucial, resulting in the interference occurring at lower harmonic orders than would be the case if the nuclei were static. For our conditions this is particularly important because it results in the interference occurring at the 39th order, rather than at the 53rd order (which is not generated in this experiment).

We also note that an SFA result considering only the modal value of the alignment distributions (Fig. 2 inset) predicts a peak ratio occurring at a time 1.38 fs after ionization. This agrees well with the time at which the simple model (Fig. 2) predicts that destructive interference will occur in H_2 (1.4 fs after ionization). However, the reason for this agreement is not clear, since the SFA result [Eq. (2)] involves an integral over R in which the integrand includes both the evolved and initial nuclear wave packets. Therefore, while it seems intuitive to use the value of R at the time of recombination in the simple model, it is not clear that this is the correct choice. Whilst we are not at present able to give a theoretical proof for this agreement, we have confirmed by calculation that it is robust with respect to changes in the laser parameters or nuclear mass. Furthermore, we have noted that the agreement is observed only when the ratio of isotopes is taken.

In conclusion, we have observed a new kind of two-center interference by studying HHG in H_2 within the PACER technique. This is a dynamic effect involving an interplay between the nuclear motion and the time-dependent nature of the returning electron wave packet. In essence, the nuclear dynamics cause the interference to occur at lower harmonic orders than would be the case for static nuclei. Thus we have been able to observe recombination interference in H_2 for the first time, in a dynamic manifestation.

This work was supported by EPSRC (Grants No. EP/C530764/1 and No. EP/E028063/1) and the Deutsche Forschungsgemeinschaft. We also thank the staff at ALLS and the Canadian Foundation for Innovation.

*sarah.baker@imperial.ac.uk

[1] R. Bartels *et al.*, Nature (London) **406**, 164 (2000).
[2] Ph. Zeitoun *et al.*, Nature (London) **431**, 426 (2004).
[3] R. Kienberger *et al.*, Nature (London) **427**, 817 (2004).
[4] Rodrigo Lopez-Martens *et al.*, Phys. Rev. Lett. **94**, 033001 (2005).
[5] G. Sansone *et al.*, Science **314**, 443 (2006).
[6] S. Baker *et al.*, Science **312**, 424 (2006).
[7] Nicholas L. Wagner *et al.*, Proc. Natl. Acad. Sci. U.S.A. **103**, 13 279 (2006).
[8] M. Lein *et al.*, Phys. Rev. A **66**, 023805 (2002).
[9] M. Lein *et al.*, Phys. Rev. Lett. **88**, 183903 (2002).
[10] R. de Nalda *et al.*, Phys. Rev. A **69**, 031804(R) (2004).
[11] J. Itatani *et al.*, Nature (London) **432**, 867 (2004).
[12] J. Itatani *et al.*, Phys. Rev. Lett. **94**, 123902 (2005).
[13] C. Vozzi *et al.*, Phys. Rev. Lett. **95**, 153902 (2005).
[14] Tsuneto Kanai, Shinichirou Minemoto, and Hirofumi Sakai, Nature (London) **435**, 470 (2005).
[15] R. Torres *et al.*, Phys. Rev. Lett. **98**, 203007 (2007).
[16] Manfred Lein, Phys. Rev. Lett. **94**, 053004 (2005).
[17] Y. Mairesse *et al.*, Science **302**, 1540 (2003).
[18] S. Baker *et al.*, J. Mod. Opt. **54**, 1011 (2007).
[19] Philippe Antoine, Anne L'Huillier, and Maciej Lewenstein, Phys. Rev. Lett. **77**, 1234 (1996).
[20] R. Torres, R. de Nalda, and J. P. Marangos, Phys. Rev. A **72**, 023420 (2005).
[21] W. A. Bryan *et al.*, Phys. Rev. A **76**, 023414 (2007).
[22] Supporting online material, S. Baker *et al.*, Science **312**, 424 (2006).
[23] G. L. Yudin and M. Y. Ivanov, Phys. Rev. A **63**, 033404 (2001).
[24] J. Levesque *et al.*, Phys. Rev. Lett. **98**, 183903 (2007).